Numerical analysis of high-frequency azimuthal oscillations in Hall thrusters

IEPC-2015-371/ISTS-2015-b-371

Presented at Joint Conference of 30th International Symposium on Space Technology and Science, 34th International Electric Propulsion Conference and 6th Nano-satellite Symposium
Hyogo-Kobe, Japan
July 4–10, 2015

Diego Escobar*
Universidad Politécnica de Madrid (UPM), Madrid, 28040, Spain

Eduardo Ahedo†
Universidad Carlos III de Madrid (UC3M), Leganés, 28911, Spain

The linear stability of the Hall thruster discharge is analysed against axial-azimuthal perturbations in the high frequency range using a time-dependent 2D code of the discharge accounting for electrons and ions. This azimuthal stability analysis is spatially global, as opposed to the more common local stability analyses. The study covers high frequency azimuthal oscillations, usually known as electron-drift waves. The influence on the electron-drift oscillations of different operation parameters of Hall thrusters such as discharge voltage and mass flow is assessed by means of different parametric variations. Comparisons against experimental results are performed to cross-check the main trends of the oscillations. Finally, an analysis is carried out of the possible contribution of these electron-drift oscillations to the anomalous diffusion present in Hall thrusters.

Nomenclature

$\mathbf{E}, \mathbf{B}$	= electric and magnetic field vectors
E, B	= electric and magnetic field magnitudes
x, r, y	= axial, radial and azimuthal coordinate
t	= time
θ	= angular azimuthal coordinate
f	= oscillation frequency
ω	= oscillation angular frequency
ω_{re}, ω_{im}	= real and imaginary parts of the angular frequency
m	= wave mode number
k	= wave number
k_x, k_y	= axial and azimuthal wave numbers
L	= typical length of axial variation of macroscopic variables
n, ν_e	= plasma density and electron collision frequency
$_{e,i}$	= subindex for electrons and ions
$\mathbf{v}_e, \mathbf{v}_i$	= electron and ion fluid velocity vectors
v_{kj}	= fluid velocity of k-th species (e, i) in the j-th direction (x, y)

*PhD Candidate, Equipo de Propulsión Espacial y Plasmas (EP2), descobar@gmv.com
†Professor, Equipo de Propulsión Espacial y Plasmas (EP2), eduardo.ahedo@uc3m.es

e, m_e, m_i = electron charge, and electron and ion masses
ϕ, T_e = electric potential and electron temperature
u = generic macroscopic variable
$u_0, \tilde{u}_1$ = zero-th and first order macroscopic variable
u_1 = Fourier coefficient of first order macroscopic variable
ω_e, ω_i = electron and ion gyro-frequencies
ω_{LH} = lower hybrid angular frequency
N = number of points in discretization
Λ = function for non-trivial solutions
$\dot{m}$ = mass flow rate through the anode
V_d = discharge voltage
L_{ch}, d_c, R = length, width and mean radius of the channel
A = cross-section of the thruster
x_{max} = location of the maximum magnetic field with respect to the anode
L_{AE} = distance from anode to external cathode
T_{eB}, T_{eE} = anode and cathode electron temperature
v_{nB} = neutral velocity at injection
α_B = anomalous diffusion coefficient
$\tilde{\nu}_w$ = dimensionless parameter for the wall losses model
T_{SEE} = electron temperature yielding 100% of secondary electron emission
a_w = accommodation factor
L_{m1}, L_{m2} = characteristic lengths of the magnetic field profile in the channel and in the plume
I_d = discharge current
v_y = oscillation phase speed
j_{ex} = electron axial density current
α_A = equivalent anomalous diffusion coefficient
I_{e1} = electron current due to oscillations

I. Introduction

Hall Effect Thrusters show a large variety of oscillations, both axial and azimuthal. Aside from low frequency oscillations such as the breathing mode or the azimuthal spoke, experiments also reveal the presence of high-frequency oscillations in the azimuthal direction[1] , usually called electron-drift oscillations.

This study is devoted to the analysis of the stability of the Hall thruster discharge against high frequency azimuthal perturbations from a global point of view. This global analysis focuses on long-wavelength high-frequency oscillations (1-10 MHz), as opposed to the analysis carried out previously focused on low frequency phenomena[58] . These high-frequency oscillations are usually referred to as electron drift waves in the Hall thruster literature as they normally rotate with a phase velocity of the order of the **E**x**B** drift (10^6m/s). Experiments with different Hall thrusters provide evidence of the presence of such azimuthal oscillations in the range of 1-10MHz with a wavelength similar to the channel perimeter[1–5] . These oscillations should not be mistaken with other high-frequency azimuthal oscillations with a much shorter wavelength, of the order of the electron gyro-radius, which are out of the scope of the current analysis. High-frequency long-wavelength oscillations have already been studied with global methods previously[4,6,7] . The current analysis extends and completes the analyses presented in those references from the following points of view.

First, all relevant terms are kept in the formulation of the theoretical model used to characterize the electron-drift oscillations. The effect of the ion species is often neglected[4] as it is assumed that the frequency of the oscillation is much higher than the lower-hybrid frequency. That condition is not strictly met and ion dynamics introduce a resonance in the dispersion relation at the lower-hybrid frequency[7] . Gradients of plasma variables are sometimes also neglected although it is believed that these terms play a role in this high-frequency regime. The study presented here includes all those terms in the formulation, even electron neutral collisions whose effect has not been analysed previously.

Secondly, an analysis of the effect on electron-drift oscillations of the different operation parameters of the Hall thruster is carried out by means of parametric variations on magnetic field, discharge voltage, and mass flow. For this purpose, zero-th order solutions obtained with the well-known 1D model of Ahedo *et al.*[8] are used. The goal here is to compare the trends seen in the numerical simulations with those observed experimentally.

And thirdly, Hall thrusters exhibit a higher-than-expected electron perpendicular conductivity. One of the plausible explanations for this excessive mobility is the existence of correlated azimuthal oscillations of electric field and plasma density. Thus, electron-drift waves may contribute to this high conductivity in the thruster. This study analyses their possible participation in the anomalous diffusion mechanism.

The paper is organized as follows. In Section II an in-depth literature review in the field of high-frequency long-wave-length azimuthal oscillations in Hall thrusters is presented. Section III is devoted to the description of the formulation used in the rest of the analyses, where the hypotheses and governing equations used are presented together with the resulting dispersion relation. In Section IV, high frequency long-wavelength azimuthal oscillations are studied with a global stability analysis and, in particular, electron-drift oscillations are studied in detail with the dispersion relation developed in the previous section. In Section V the possible contribution of electron-drift oscillations on electron conductivity is evaluated and discussed. Finally, Section VI is devoted to conclusions.

II. Literature review

A. Experimental results

In the 1970's azimuthal high frequency oscillations with a phase velocity close to the **E**x**B** drift were proposed theoretically and later on detected experimentally by Esipchuk and Tilinin[2] . Those oscillations appear in the region of negative magnetic field gradient as long wavelength oscillations that rotate with no phase shift along the thruster. Tilinin[9] continued with the analysis of these high frequency waves, confirming their previous findings and obtaining further insights about their properties that can be summarized as: decreasing intensity with increasing frequency, significant dependence on the operation point and increasing amplitude with the magnetic field.

At the end of the 1990's and the beginning of the 2000's, the interest in the high-frequency spectrum gained inertia again and several experimental studies have been carried out with modern Hall thrusters ever since. In particular, Guerrini *et al.*[3] detect azimuthal oscillations in the near field of a SPT-50 within the 1-10 MHz range using Langmuir probes. With a similar experimental set-up and a 900 W laboratory Hall thruster, Litvak *et al.*[10,11] observe intermittent signals of a few MHz with an azimuthal phase velocity close to the electron drift and a wave mode $m = 1$. All these oscillations seem to correspond to the electron drift waves proposed by Esipchuk and Tilinin. The frequency of the oscillation varies significantly with the operating point of the thruster since the electron drift velocity is directly proportional to the electric field and inversely proportional to the magnetic field. An interesting conclusion of the analysis of Litvak *et al.* is the fact that the velocity of the wave is not equal to the local value of the **E**x**B** drift, and at the same time is constant along the thruster. These facts point to a non-local instability mechanism. Additionally, Litvak *et al.* also observe oscillations of higher wave-numbers that are independent of the $m = 1$ oscillation.

Lazurenko *et al.* have performed a series of detailed studies on the high-frequency spectrum of two laboratory thrusters of different size and power, SPT-100-ML and PPS-X000-ML, using various experimental techniques, intrusive and non-intrusive: isolated antennas, magnetic coils and electrostatic probes[12–20] . As a summary of those analyses, Lazurenko *et al.*[20] present the main properties of the high-frequency signals, in good agreement with the work of Esipchuk *et al.* , Guerrini *et al.* and Litvak *et al.*:

1. *frequency of a few MHz (1-10 MHz) and fundamental mode* $m = 1$: the instability can evolve into more complex structures with several superimposed $m = 1$ signals and/or higher harmonics.

2. *azimuthal propagation*: the oscillations propagate mostly azimuthally in the near field of the thruster, this is, from the magnetic field maximum to a distance of a few cm from the thruster exit. Axial oscillations in this frequency range are also observed inside the thruster and further downstream of the near field.

3. *intermittency*: high-frequency bursts take place only during the descent part of the discharge current of the breathing mode oscillations.

4. *electron drift velocity*: the phase velocity of the azimuthal waves is close to the **E**x**B** drift and, more importantly, constant along the thruster.

5. *azimuthal asymmetry*: the azimuthal velocity of the wave is not axi-symmetric, possibly due to an asymmetry of the electric field, which, in turn, may be caused by the presence of the cathode.

6. *variation of the velocity over time*: the observed velocity of the instability increases from the onset to the disappearance of the wave as a consequence of the variation of the electric field over the breathing mode period.

7. *gradient induced waves*: based on the previous properties, Lazurenko suggests that these signals correspond to the fluctuations induced by magnetic field and density gradients proposed by Morozov[21] and Esipchuk and Tilinin[2] rather than the resistivity instabilities suggested by Litvak *et al.*[22] .

8. *maximum frequency in optimized operation*: as the mass flow changes over different operating points and the magnetic field is optimized accordingly, the frequency of the instability remains constant and maximal.

9. *small azimuthal extension*: it is estimated that the size of the wave is one order of magnitude smaller than the channel circumference.

10. *linear azimuthal dispersion relation*: experiments show a nearly linear relation between the frequency and the wave number of the oscillation.

Knoll *et al.*[5,23] confirm several of the previous properties in a experimental study carried out with a laboratory Hall thruster and a group of three Langmuir probes separated axially and azimuthally. This experimental set-up allows the detection of axial and azimuthal waves and its variation with the axial location. The results of the analysis also reinforce the idea of a non-local instability due to the constant azimuthal speed of the oscillations. Interestingly, in this work it is also pointed out that the velocity of the azimuthal waves is consistently smaller than the electron drift velocity and thus different growth mechanisms than those indicated by Lazurenko are suggested. More recently, Tomilin[24] has detected high frequency oscillations of similar properties in a SPT Hall thruster with high specific impulse.

On the other hand, Albarede *et al.*[25] analyse low frequency processes and how they are related to the high frequency oscillations. In particular, as a consequence of the breathing mode, the maximum of plasma density and the minimum of electric potential in the near field plume take place at the same time as the high frequency bursts. According to Albarede *et al.* , this fact supports the idea that the cathode dynamics and the beam neutralization process might promote high-frequency signals.

Another interesting set of experimental studies are those carried out by Kurzyna *et al.*[26–28] and Bonhomme *et al.*[29,30] . In these studies, a novel technique called Empirical Mode Decomposition is used to analyse the signals obtained from experiments. This method, even though lacking a strong mathematical foundation, is particularly well suited for the analysis of non-stationary signals. For such cases, Fourier analysis tends to fail because of the intermittency of the signals. In the first of those researches[26] a thorough evaluation is carried out of the different oscillations detected with that technique. The usual oscillations (breathing mode, transit-time and electron drift oscillations) are cleanly filtered and observed. In a later research, the variation of the oscillations with the operating point is considered. It turns out that at high voltage the breathing mode almost disappears and transit time oscillations become dominant. And more interestingly, high-frequency bursts appear now during the descent part of the transit time oscillations, what points to the idea of a coupling between the dominating medium frequency oscillation and the high frequency waves.

In line with previous numerical results[31–33] , in a series of experiments, first Adam *et al.*[34] and later on Tsikata *et al.*[35–38] , have detected high frequency and short wavelength azimuthal oscillations via collective light scattering, a technique commonly used in nuclear fusion researches. The experiments confirm the presence at the thruster exit of oscillations of a few MHz (1-10 MHz) with a wavelength of the order of the electron Larmor radius (1 mm) and a phase velocity of a few km/s, which is close to the ion acoustic velocity. The results seem to indicate that the propagation velocity has a small component in the axial direction towards the anode. Given the short wavelength of these oscillations and the mechanism based on the interaction between the electron gyro-motion and electric field oscillations, it is clear that these oscillations cannot be analysed with typical fluid equations.

B. Numerical results

Hirakawa *et al.*[39,40] implemented the first azimuthal numerical code for the analysis of oscillations using a particle-in-cell method. In that numerical study, high frequency oscillations were observed propagating in the **E**x**B** direction and enhancing the electron mobility, which turned out to be of the order of the Bohm diffusion. However, that study does not reproduce the variation of the Hall parameter along the thruster and, in particular, the presence of a dip of mobility around the thruster, which is one of the key properties of the anomalous diffusion[41] .

As already mentioned, Adam *et al.*[31] have implemented a full PIC simulation code in two dimensions $(r-\theta)$. Even though the computational cost is enormous, some results have been obtained for a reduced and simplified geometry. The model does not require adding any artificial diffusion thanks to the presence of azimuthal high frequency waves that enhance the cross-field electron mobility. These waves have a wavelength close to the electron Larmor radius and propagate with a velocity of a few km/s. According to the simulations, the density variations introduced by the waves can be even higher than the average value in some parts of the thruster. Moreover, the growth of this type of oscillations is supported by the stability analysis carried out by Ducrocq *et al.*[42] , who make use of a kinetic model for electrons rather than the conventional fluid approach. Furthermore, there are experimental results confirming the existence of these type of oscillations. These waves could correspond to those detected by Tsikata *et al.*[36,38] . Further numerical analyses following the work of Adam *et al.* have been presented recently[43,44] and similar results are obtained by Coche and Garrigues with an independent PIC code[32,33] .

Lately, some other bi-dimensional numerical codes have been developed. Lam *et al.*[45] , apart from a hybrid $r-\theta$ code, have implemented in parallel a fully fluid simulation code following the preliminary work of Knoll *et al.*[46] . With this code, Lam *et al.* predict tilted waves at 5 MHz with a mode number of $m = 3$ travelling in the -**E**x**B** direction with a phase velocity of 300 km/s. The presence of these waves gives the required conductivity to the electron flow and makes it unnecessary to introduce artificial mobility in the simulation. However, there are two arguments against this result worth mentioning: in first place, experiments normally detect high frequency azimuthal waves only in the near field plume; and, in second place, the simulated waves propagate in the opposite direction to what is normally measured.

C. Theoretical models

Esipchuk and Tilinin[2] predict, apart from the low frequency oscillation already mentioned above, a high frequency wave of the electron-drift type. The inclusion of electron inertia terms in the governing equations is the key to turn the dispersion relation into a cubic equation for the frequency. If the electron inertia is neglected, the dispersion relation reduces to a quadratic equation whose solutions are in the medium frequency range. If not, roots of the cubic equation can appear in the high frequency range, close to the lower hybrid frequency, for certain combinations of the parameters of the model.

In a series of studies[47–49] , Baranov *et al.* analyse separately the stability of the different regions of the thruster accounting for different effects in each of them: temperature terms and zero electric field in the ionization region, and strong electric and magnetic fields in the acceleration region. The results show azimuthal waves of high frequency both in the ionization and acceleration regions. In the case of the ionization region, the temperature seems to be the driving force. However, there is no experimental evidence of the existence of such high frequency azimuthal waves in the rear part of the thruster. Besides, no ionization terms and neutral gas equations are considered in the model and therefore, low frequency phenomena are not taken into account.

Litvak *et al.*[22] focus on the effect of the electron collisions on the stability of the discharge. In their research, two types of unstable azimuthal oscillations appear: an electrostatic instability and an electromagnetic one. Both are promoted by the electron collisionality, but the former rotates with a frequency close to the lower hybrid frequency (10 MHz) while the latter propagates at the Alfven speed with a frequency of 1 MHz. According to the analysis, the higher growth rate of the electrostatic oscillation makes it more likely.

A formalism to analyse the linear stability of a two-fluid electrostatic model of the Hall discharge is presented by Thomas *et al.*[50,51] The result in the no-gradients limit coincides with the expression of Baranov *et al.*[47] , but the analysis is extended to account for electron-drift shear, electron-neutral collisions and electron temperature by means of an equation of state. The resulting dispersion relation is applied to the experimental profiles of a laboratory thruster and the results indicate the presence of unstable oscillations in the high frequency range above 1 MHz.

Spektor[52] uses a linear stability method including collisions, macroscopic gradients and temperature terms to derive a dispersion relation that is used in turn to compute the equivalent anomalous electron collision frequency from plasma susceptibility. This approach has been successfully applied in the area of MPD thrusters to characterize the electron conductivity in those devices, but in the case of Hall thrusters, the results obtained by Spektor predict an anomalous diffusion scaling as $1/B^4$. Clearly, this relation is against the experimentally verified scaling law for the Bohm diffusion[53] of $1/B$.

On the other hand, Ducrocq *et al.*[42,54,55] use a kinetic model to describe the electron species. In this research an electron drift instability of short wave-length, close to the electron Larmor radius (1 mm), and high frequency (1-10 MHz), is predicted as a result of a resonance between the gyro-motion of the electrons and oscillations of the electric field. This analysis agrees with the numerical results of Adam *et al.*[31] and Coche and Garrigues[32,33] obtained with different PIC codes.

A second way to study the stability of the discharge is based on a global approach. It involves analysing the eigenvalue problem obtained when the axial coordinate is not resolved in the usual exponential form (i.e., $\exp(ik_x x)$). This method is used by Kapulkin *et al.* in several studies[6,7,56,57] as well as by Litvak *et al.*[4] . The same approach is used in classical fluid mechanics to study the well known Rayleigh instability and hence the name of Rayleigh type of instabilities in Hall thrusters. The main advantage of this method over the previous one is that the former is based on a local analysis, while with the latter approach the stability of the discharge is analysed globally. Moreover, it has been observed experimentally that the velocity of high-frequency azimuthal waves is constant along the near field plume. This fact points to a non-local mechanism and supports the use of more elaborated stability methods such as those used by Kapulkin and Litvak.

Kapulkin *et al.*[6,56] and Litvak *et al.*[4] conclude separately that Rayleigh type of instabilities appear inside the Hall thruster with frequencies higher than the lower hybrid frequency. In both researches, the phase speed of the unstable wave is of the order of the ratio E_{max}/B_{max}. Moreover, the exact value of the wave velocity coincides with the electron drift at a given point along the thruster. The influence of the density and magnetic field gradients is highlighted by both authors: the higher the gradients are, the lower the frequency of the wave is. As a consequence of the instability, the electric potential fall is spread out along the thruster reducing the maximum electric field. However, it is important to remark that these analyses focus on a frequency range above the hybrid lower frequency (1-10 MHz), which is where high frequency oscillations are normally detected experimentally.

In a another study, Kapulkin *et al.*[7] analyse waves in the lower-hybrid frequency range with the same approach. The main novelty with respect to the previous study is the inclusion of the ion dynamics. As a result, a resonant effect at the lower hybrid frequency appears in the dispersion equation. However, the main driver for the instability is the same as before, the electron drift velocity non-uniformity. This theoretical instability has several properties in common with those measured experimentally: azimuthal propagation in the direction of the electron drift, frequency of around 1 MHz and wavelength of the order of the channel circumference.

D. Conclusions from the literature review

To sum up, long wavelength high-frequency oscillations have been detected by several researchers by means of different experimental techniques in Hall thrusters of various kinds and sizes. Thus, it seems clear that the presence of these oscillations is an essential property of the physics involved in Hall thrusters, rather than a particular feature of a given model. Their intensity makes it reasonable to propose a relation with the anomalous electron conductivity. However, it is only at the thruster exit that these oscillations are azimuthal. Thus, it is not possible to explain the high electron current in the channel based only on these oscillations. In that part of the thruster there must be another mechanism enhancing the electron cross-field mobility.

On the other hand, short-wavelength high-frequency oscillations have also been observed experimentally via collective light-scattering techniques, and there are numerical results and analytical theories supporting the presence of those oscillations. Moreover, a relation with enhanced electron mobility has also been established theoretically and numerically. Thus, these oscillations seem to be also a relevant aspect of the anomalous diffusion mechanism.

III. Formulation

This section is intended to present the formulation used for the analysis of high-frequency long-wavelength azimuthal oscillations. In first place, the main hypotheses and resulting governing equations are presented and then the final dispersion relation is derived and compared against previous studies.

A. Main hypotheses and governing equations

Fluid equations are used to model the different species under consideration. As the focus is on the high-frequency range (1-10MHz), certain hypotheses that greatly simplify the formulation can be made. On the other hand, many of the hypotheses employed for the derivation of the 1D model of Ahedo *et al.*[8] and of a 2D linear model developed previously[58] are applied here as well. The following hypotheses are additionally considered for the perturbation model, compared to those used for the low frequency first order formulation:

- Perturbations of ionization or particle wall-recombination are not included in the model as those are low frequency phenomena not affecting the high-frequency range under study. This allows reducing the problem to a two-fluid model without neutral equations.
- Electron inertia terms are kept in the formulation, as they are critical for the promotion of electron-drift oscillations.
- No electron temperature perturbations are considered since it is believed that the electron temperature plays no role at this high-frequency range. This assumption allows removing the electron energy equation from the model.
- Only 2D effects are considered, in the axial and azimuthal directions (x and y), and curvature effects and variations in the radial direction are neglected.
- Plume divergence is neglected as it is thought it has no effect on electron-drift waves.
- The following ordering for the frequencies is considered:
$$\omega_e \gg \omega \sim k v_{ey0} \gg v_{ix0}/L \sim k v_{ex0} \tag{1}$$
where $\omega_e = eB_0/m_e$ is the electron gyro-frequency, L is the typical length of variation of macroscopic variables in the axial direction, verifying $L/R \sim 1$ with R the channel mean radius, k is the oscillation wave number, verifying $kL \sim 1$, and the rest of symbols as usual.

With these assumptions, the resulting 2D model consists of continuity and momentum equations of electrons and ions, which are expressed in non-conservative form as:

$$\frac{\partial n}{\partial t} + \nabla \cdot (n\mathbf{v}_e) = \frac{\partial n}{\partial t} + \nabla \cdot (n\mathbf{v}_i) = 0 \tag{2a}$$

$$m_e n \left(\frac{\partial \mathbf{v}_e}{\partial t} + \mathbf{v}_e \cdot \nabla \mathbf{v}_e \right) = -en(-\nabla\phi + \mathbf{v}_e \times \mathbf{B}) - m_e n \nu_e \mathbf{v}_e \tag{2b}$$

$$m_i n \left(\frac{\partial \mathbf{v}_i}{\partial t} + \mathbf{v}_i \cdot \nabla \mathbf{v}_i \right) = -en\nabla\phi \tag{2c}$$

where t is the time variable; n is the plasma density; $\mathbf{v}_e$ and $\mathbf{v}_i$ are the fluid velocities of electrons and ions; $\mathbf{E}$ and $\mathbf{B}$ are the electric and magnetic fields; m_i and m_e are the ion and electron masses; e is the electron charge; and ν_e is the electron collision frequency. Note that as in the 1D model of Ahedo *et al.* the induced magnetic field is neglected and thus, Maxwell's equations are not included in the model. Therefore, the magnetic field is equal to the field externally applied, which is stationary, solenoidal, irrotational and mostly radial. Consequently, the electric field derives from an electric potential ($\mathbf{E} = -\nabla\phi$) and the formulation is electrostatic. This simplification is valid even in this relatively high-frequency regime under analysis (1-10MHz)as shown by Esipchuk and Tilinin[2] .

Note that Eqs. (2) are only used for the perturbation model and the derivation of the dispersion relation of the first order problem. The background state, whose stability is analysed, is computed with the 1D model of Ahedo *et al.*[8] . The fact that the zero-th and first order solutions are computed considering different effects does not imply any inconsistency since each of the models needs to take into account different physical aspects of the Hall discharge.

B. Linearised formulation

Let us assume that any macroscopic variable, say $u(x,y,t)$, may be written as the sum of an axially-dependent zero-th order solution, $u_0(x)$, and a small perturbation, $\tilde{u}_1(x,y,t)$. Making use of the small perturbations hypothesis ($u_0 \gg \tilde{u}_1$) and applying the frequency ordering given in Eq. (1), Eqs. (2) can be linearised as follows:

$$\frac{\partial \tilde{n}_1}{\partial t} + n_0\left(\frac{\partial \tilde{v}_{ex1}}{\partial x} + \frac{\partial \tilde{v}_{ey1}}{\partial y}\right) + \tilde{v}_{ex1}\frac{dn_0}{dx} + v_{ey0}\frac{\partial \tilde{n}_1}{\partial y} = 0 \tag{3a}$$

$$\frac{\partial \tilde{n}_1}{\partial t} + n_0\left(\frac{\partial \tilde{v}_{ix1}}{\partial x} + \frac{\partial \tilde{v}_{iy1}}{\partial y}\right) + \tilde{v}_{ix1}\frac{dn_0}{dx} = 0 \tag{3b}$$

$$\frac{\partial \tilde{v}_{ex1}}{\partial t} + v_{ey0}\frac{\partial \tilde{v}_{ex1}}{\partial y} = -\frac{e}{m_e}\left(-\frac{\partial \tilde{\phi}_1}{\partial x} + \tilde{v}_{ey1}B_0\right) - \nu_{e0}\tilde{v}_{ex1} \tag{3c}$$

$$\frac{\partial \tilde{v}_{ey1}}{\partial t} + v_{ey0}\frac{\partial \tilde{v}_{ey1}}{\partial y} + \tilde{v}_{ex1}\frac{dv_{ey0}}{dx} = -\frac{e}{m_e}\left(-\frac{\partial \tilde{\phi}_1}{\partial y} - \tilde{v}_{ex1}B_0\right) - \nu_{e0}\tilde{v}_{ey1} \tag{3d}$$

$$\frac{\partial \tilde{v}_{ix1}}{\partial t} = -\frac{e}{m_i}\frac{\partial \tilde{\phi}_1}{\partial x} \tag{3e}$$

$$\frac{\partial \tilde{v}_{iy1}}{\partial t} = -\frac{e}{m_i}\frac{\partial \tilde{\phi}_1}{\partial y} \tag{3f}$$

where perturbations of the electron collisional frequency, ν_e, are not considered.

The perturbations can be Fourier-expanded in t and y and, then, the complete solution may be expressed as:

$$u(x,y,t) = u_0(x) + \Re\left\{u_1(x;\omega,k)\exp(-i\omega t + iky)\right\} \tag{4}$$

where $\omega = \omega_{re} + i\omega_{im}$ is the complex angular frequency and k is the wave number of the oscillation.

If that Fourier form is assumed for all perturbations, then, it is possible to re-write Eqs. (3) in the following form:

$$-i\omega n_1 + n_0\left(\frac{dv_{ex1}}{dx} + ikv_{ey1}\right) + v_{ex1}\frac{dn_0}{dx} + v_{ey0}ikn_1 = 0 \tag{5a}$$

$$-i\omega n_1 + n_0\left(\frac{dv_{ix1}}{dx} + ikv_{iy1}\right) + v_{ix1}\frac{dn_0}{dx} = 0 \tag{5b}$$

$$-i\omega v_{ex1} + v_{ey0}ikv_{ex1} = -\frac{e}{m_e}\left(-\frac{d\phi_1}{dx} + v_{ey1}B_0\right) - \nu_{e0}v_{ex1} \tag{5c}$$

$$-i\omega v_{ey1} + v_{ey0}ikv_{ey1} + v_{ex1}\frac{dv_{ey0}}{dx} = -\frac{e}{m_e}\left(-ik\phi_1 - v_{ex1}B_0\right) - \nu_{e0}v_{ey1} \tag{5d}$$

$$-i\omega v_{ix1} = -\frac{e}{m_i}\frac{d\phi_1}{dx} \tag{5e}$$

$$-i\omega v_{iy1} = -\frac{e}{m_i}ik\phi_1 \tag{5f}$$

Based on Eqs. (5c), and (5d), the following expressions result for the electron velocity perturbations:

$$v_{ex1} \simeq \frac{e/m_e}{\omega_e^2}\left[(-i\omega + ikv_{ey0} + \nu_{e0})\frac{d\phi_1}{dx} - \left(\omega_e + \frac{dv_{ey0}}{dx}\right)ik\phi_1\right] \tag{6a}$$

$$v_{ey1} \simeq \frac{e/m_e}{\omega_e^2}\left[\omega_e\frac{d\phi_1}{dx} + (-i\omega + ikv_{ey0} + \nu_{e0})ik\phi_1\right] \tag{6b}$$

where terms of second order or higher in ω/ω_e, kv_{ey0}/ω_e or ν_{e0}/ω_e have been neglected.

From Eqs. (5a) and (6), the following expression results for the plasma density perturbation:

$$\frac{n_1}{n_0} \simeq -\frac{e/m_e}{\omega_e^2}\left[\left(\frac{d^2\phi_1}{dx^2} - k^2\phi_1 + \frac{d\phi_1}{dx}\frac{d}{dx}\ln\frac{n_0}{B_0^2}\right)\left(1 + \frac{\nu_{e0}}{-i\omega + ikv_{ey0}}\right) + \right.$$
$$\left. + \frac{ik\phi_1}{-i\omega + ikv_{ey0}}\left(-\omega_e\frac{d}{dx}\ln\frac{n_0}{B_0} - \frac{d^2v_{ey0}}{dx^2} - \frac{dv_{ey0}}{dx}\frac{d}{dx}\ln\frac{n_0}{B_0^2}\right)\right] \tag{7}$$

And from Eqs. (5b), (5e) and (5f), it is possible to derive the following expression for the plasma density perturbation:

$$\frac{n_1}{n_0} = -\frac{e/m_i}{\omega^2}\left[\frac{d^2\phi_1}{dx^2} - k^2\phi_1 + \frac{d\phi_1}{dx}\frac{d}{dx}\ln n_0\right] \tag{8}$$

Finally, from Eqs. (7) and (8), the following dispersion relation is obtained for the angular oscillation frequency, ω, as a function of the background state and the wave number, k:

$$(\omega^2 - \omega_{LH}^2)(\omega - kv_{ey0})\left(\frac{d^2\phi_1}{dx^2} - k^2\phi_1\right) + \omega^2 k\phi_1\frac{d^2v_{ey0}}{dx^2} +$$
$$+\omega^2\omega_e k\phi_1\frac{d}{dx}\ln\frac{n_0}{B_0} + \omega^2\left((\omega - kv_{ey0})\frac{d\phi_1}{dx} + k\phi_1\frac{dv_{ey0}}{dx}\right)\frac{d}{dx}\ln\frac{n_0}{B_0^2} + \tag{9}$$
$$+\omega^2(-i\nu_{e0})\left(\frac{d^2\phi_1}{dx^2} - k^2\phi_1 + \frac{d\phi_1}{dx}\frac{d}{dx}\ln\frac{n_0}{B_0^2}\right) = 0$$

where $\omega_{LH} = (\omega_i\omega_e)^{1/2}$ is the lower hybrid frequency with $\omega_i = eB_0/m_i$ the ion gyro-frequency. Three different types of terms are identified in Eq. (9):

1. The first row consists of the base terms, including the inhomogeneity of the electron azimuthal velocity, d^2v_{ey0}/dx^2. The effect of the ion dynamics also appears in the first row through the ion gyro-frequency, ω_i, which introduces a resonance in the dispersion relation at the lower hybrid frequency, ω_{LH}.

2. The second row corresponds to the terms due to the inhomogeneities of plasma density and magnetic field ($d/dx\ln n_0/B_0^2$, $d/dx\ln n_0/B_0$), which are sometimes negligible with respect to the electron azimuthal velocity gradient. Out of those, the dominant term is the one proportional to the electron gyro-frequency, ω_e, which is of the order of 1GHz, as opposed to the frequency range under analysis, 1-10MHz. This compensates the fact that the gradients of plasma density and magnetic field are usually smaller than that of the electron azimuthal velocity.

3. Finally, the third row contains the influence of electron collisions in the high-frequency global stability. Note that the effect from electron collisions is somehow affected by the addition of anomalous diffusion in the effective electron collisions frequency, ν_e, as part of the background solution.

Eq. (9) is a dispersion relation for the oscillation frequency consisting of a second order ordinary differential equation. It thus requires two boundary conditions, which are normally chosen as $\phi_1 = 0$ in the extremes of the simulation domain[4,7] . Note that it is implicitly assumed that no external perturbation is applied on the discharge voltage since the goal of the current analysis is the detection of self-excited unstable azimuthal oscillations. The differential dispersion relation in Eq. (9), together with its boundary conditions, is a cubic eigenvalue problem for the angular oscillation frequency, ω, as a function of the background state and the oscillation wave number, k.

In order to solve that differential eigenvalue problem, a standard approach is used. First, it is necessary to discretize the domain and then evaluate the dispersion relation at each of the points of the discretization, approximating the first and second order spatial derivatives of ϕ_1 with finite differences. This approach yields N relations, where N is the number of points of the discretization, which altogether can be expressed as a cubic algebraic eigenvalue problem for the oscillation frequency, with eigenvectors of N components corresponding to the value of ϕ_1 at each point of the discretization. This cubic algebraic eigenvalue problem can be easily transformed into a linear one at the expense of multiplying its size by a factor of 3, using as components of the eigenvectors the value of ϕ_1, $\omega\phi_1$, and $\omega^2\phi_1$ at each point. The resulting linear system can then be solved with standard methods for algebraic linear eigenvalue problems.

C. Comparison with previous dispersion relations

High-frequency oscillations have already been studied in the past with global methods[4,6,7] and different dispersion relations have been derived as part of those analyses. This section compares those dispersion relations against the one developed in the previous section. The dispersion relation in Eq. (9), apart from the base terms, contains other terms (ion dynamics, plasma density and magnetic field gradients, and electron collisions) and depending on which of those terms are kept in the formulation different dispersion relations are obtained.

If gradients of plasma density and magnetic field are completely neglected, ion dynamics are not included in the model ($\omega_i = 0$), and electron collisions are neglected (ν_{e0}), then, the simplest form of the dispersion relation in Eq. (9) is:

$$(\omega - kv_{ey0})\left(\frac{d^2\phi_1}{dx^2} - k^2\phi_1\right) + k\phi_1\frac{d^2v_{ey0}}{dx^2} = 0 \tag{10}$$

Eq. (10) is equivalent to Eq. (6) of Kapulkin *et al.*[6] , and resembles the Rayleigh equation of fluid dynamics, hence, the name of Rayleigh-type oscillations in Hall thrusters. Due to the properties of Rayleigh-type equations[4] , the condition for the existence of non-trivial solutions is that at least one point verifying $d^2v_{ey0}/dx^2 = 0$ exists. In such case, the phase speed of the solution of Eq. (10) corresponds to the azimuthal electron velocity where the previous condition is verified.

If on top of the previous equation consisting of the base terms, the term proportional to the electron gyro-frequency, ω_e, due to the gradients of plasma density and magnetic field is kept in the formulation, then, the dispersion relation in Eq. (10) results in:

$$(\omega - kv_{ey0})\left(\frac{d^2\phi_1}{dx^2} - k^2\phi_1\right) + k\phi_1\frac{d^2v_{ey0}}{dx^2} + \omega_e k\phi_1\frac{d}{dx}\ln\frac{n_0}{B_0} = 0 \tag{11}$$

Eq. (11) is equivalent to Eq. (28) of Litvak *et al.*[4] . With respect to Eq. (10), the solution of the dispersion relation in Eq. (11) is affected by the term proportional to ω_e. The equivalence with Rayleigh equation is still feasible if the following function is defined:

$$\Lambda(x) = -\omega_e\frac{d}{dx}\ln\frac{n_0}{B_0} - \frac{d^2v_{ey0}}{dx^2} \tag{12}$$

In this case the condition $\Lambda(x) = 0$ is necessary in order to have non-trivial solutions[4] . And the phase speed of the oscillation corresponds to the azimuthal electron velocity at the location where that condition is fulfilled.

In case all terms due to the gradients of plasma density and magnetic field are kept in the formulation, Eq. (11) transforms into:

$$\begin{aligned}(\omega - kv_{ey0})\left(\frac{d^2\phi_1}{dx^2} - k^2\phi_1\right) + k\phi_1\frac{d^2v_{ey0}}{dx^2} + \\ +\omega_e k\phi_1\frac{d}{dx}\ln\frac{n_0}{B_0} + \left((\omega - kv_{ey0})\frac{d\phi_1}{dx} + k\phi_1\frac{dv_{ey0}}{dx}\right)\frac{d}{dx}\ln\frac{n_0}{B_0^2} = 0\end{aligned} \tag{13}$$

Eq. (13) is equivalent to Eq. (5) of Kapulkin *et al.*[6] .

If on top of the base terms the dynamics of ions are kept, the dispersion relation in Eq. (10) is transformed into:

$$(\omega^2 - \omega_{LH}^2)(\omega - kv_{ey0})\left(\frac{d^2\phi_1}{dx^2} - k^2\phi_1\right) + \omega^2 k\phi_1\frac{d^2v_{ey0}}{dx^2} = 0 \tag{14}$$

Eq. (14) is equivalent to Eq. (4) of Kapulkin *et al.*[7] . Eq. (14) has two possible resonances at $d^2v_{ey0}/dx^2 = 0$. These correspond to the lower hybrid frequency ($\omega = \omega_{LH}$) and the electron drift ($\omega = kv_{ey0}$). The oscillation frequency thus depends on which of those resonances take place, what in turn depends on the shape and size of the profiles of ω_{LH} and v_{ey0}. In fact, this is in agreement with experimental evidence of two different ranges for the phase speed and oscillation frequency of electron drift-waves, one close to the electron azimuthal velocity, as detected by Esipchuk and Tilinin[2] , Litvak *et al.*[4] , and Lazurenko *et al.*[1] , and another one well below the electron-drift and closer to the lower hybrid frequency, as detected by Knoll *et al.*[5] .

If ion dynamics and the term proportional to ω_e due to the gradients of plasma density and magnetic field are kept, then, the dispersion relation results in:

$$(\omega^2 - \omega_{LH}^2)(\omega - kv_{ey0})\left(\frac{d^2\phi_1}{dx^2} - k^2\phi_1\right) - \omega^2 k\phi_1\Lambda = 0 \tag{15}$$

As Eq. (14), the dispersion relation in Eq. (15) has also two resonances at $\Lambda = 0$.

If both ion dynamics and electron collisions are considered, but the only term that is kept due to the gradients of plasma density and magnetic field is the one proportional to ω_e, then, the dispersion relation results in:

$$\begin{aligned}(\omega^2 - \omega_{LH}^2)(\omega - kv_{ey0})\left(\frac{d^2\phi_1}{dx^2} - k^2\phi_1\right) + \omega^2 k\phi_1\frac{d^2v_{ey0}}{dx^2} + \\ +\omega^2\omega_e k\phi_1\frac{d}{dx}\ln\frac{n_0}{B_0} + \\ +\omega^2(-i\nu_{e0})\left(\frac{d^2\phi_1}{dx^2} - k^2\phi_1 + \frac{d\phi_1}{dx}\frac{d}{dx}\ln\frac{n_0}{B_0^2}\right) = 0\end{aligned} \tag{16}$$

Eq. (16) is equivalent to Eq. (27) of Litvak *et al.*[4] .

In case all elements are considered in the formulation (gradients, ion dynamics, electron collisions), the dispersion relation is the one given in Eq. (9). In this case, due the different terms included, it is not possible to establish a direct equivalence with the Rayleigh equation, as there are elements proportional to $d\phi_1/dx$ in the dispersion relation, which do not appear in the Rayleigh equation.

On the other hand, the form of the simplistic dispersion relation in Eq. (10) ensures that if ω is an eigenvalue for a given k, then, $n\omega$ is also an eigenvalue for the wave number nk, where n is any integer. This can be easily verified by transforming Eq. (9) to non-dimensional space using $1/k$ as reference length. This means that the dispersion relation for ω is linear in terms of k and that the phase speed is constant when the wave number is modified, facts that have been observed experimentally[1] .

To sum up, the original dispersion relation in Eq. (9) combines all effects and reduces to the ones existing in the literature of global methods for high-frequency oscillations in Hall thrusters in the corresponding limits. In this sense, the relation derived as part of this work may be understood as a general case of the different dispersion relations developed in the past.

In the limit of diffusive electrons ($m_e = 0$), the dominant terms in the dispersion relation are those proportional to ω_e, and the dispersion relation in Eq. (9) simplifies to:

$$\omega_i(\omega - kv_{ey0})\left(\frac{d^2\phi_1}{dx^2} - k^2\phi_1\right) - \omega^2 k\phi_1\frac{d}{dx}\ln\frac{n_0}{B_0} = 0 \tag{17}$$

The dispersion relation in Eq. (17) is somehow similar to the Rayleigh equation and the necessary condition for the existence of non-trivial solutions can be expressed as:

$$\frac{d}{dx}\ln\frac{n_0}{B_0} = 0 \tag{18}$$

The condition in Eq. (18) contrasts with the one in Eq. (10) when ion dynamics and gradients are neglected ($d^2v_{ey0}/dx^2 = 0$). In the general case a combination of those two terms appear in the formulation to require the condition $\Lambda = 0$ mentioned above.

Moreover, the *local* stability analysis of Esipchuk and Tilinin[2] in the limit of diffusive electrons predicts unstable oscillations in regions where $d/dx(\ln n_0/B_0) > 0$. The condition given by Eq. (18) is only a necessary condition for the existence of non-trivial solutions, but it does not say anything about where those unstable oscillations are located. However, for a Rayleigh-type equation and an azimuthal electron velocity monotonically increasing with x, in order to have unstable solutions Fjortoft's theorem requires that $d/dx(\ln n_0/B_0) > 0$ when $x > x_0$, being x_0 the location where the condition $d/dx(\ln n_0/B_0) = 0$ is satisfied. This condition that is normally met by the profile of n_0 and B_0 in the acceleration region, where high frequency oscillations are normally measured.

Finally, there is yet another limit of interest obtained for purely axial oscillations ($k = 0$). In that limit, the dispersion relation reduces to:

$$(\omega^2 - \omega_{LH}^2)\frac{d^2\phi_1}{dx^2} + \omega^2\frac{d\phi_1}{dx}\frac{d}{dx}\ln\frac{n_0}{B_0^2} + \omega(-i\nu_{e0})\left(\frac{d^2\phi_1}{dx^2} + \frac{d\phi_1}{dx}\frac{d}{dx}\ln\frac{n_0}{B_0^2}\right) = 0 \tag{19}$$

In case electron collisions and ion dynamics are neglected for axial oscillations, there are no unstable solutions to the resulting dispersion relation. However, if ion dynamics are kept, Eq. (19) simplifies to:

$$(\omega^2 - \omega_{LH}^2)\frac{d^2\phi_1}{dx^2} + \omega^2 \frac{d\phi_1}{dx}\frac{d}{dx}\ln\frac{n_0}{B_0^2} = 0 \tag{20}$$

Eq. (20) has a resonance at the lower hybrid frequency, ω_{LH}, which requires the condition $d/dx(\ln n_0/B_0^2) = 0$ at the same location in order to avoid singularities.

These last dispersion relations corresponding to purely axial oscillations ($k = 0$) could model the high-frequency axial waves observed in experiments of Hall thrusters inside the channel[3,5] .

IV. Results and discussion

This section is devoted to the presentation and discussion of the results obtained with the high-frequency dispersion relation developed in the previous section for different background states obtained with the 1D model of Ahedo *et al.*[59] , including heat conduction and plume divergence. First, results for a reference background state are analysed and then, results for selected cases with different operating conditions are discussed. For completeness, a description of the different operating conditions considered is presented in the following paragraphs.

The reference background state corresponds to a SPT-100 thruster whose main simulation parameters are presented in Table 1 . The following symbols are used: $\dot{m}$ is the mass flow rate through the anode; V_d is the discharge voltage; B_{max} is the maximum magnetic field; x_{max} is the location of the maximum magnetic field with respect to the anode; L_{AE} is the distance from anode to external cathode; L_{ch}, d_c and R are respectively the length, width and mean radius of the channel; T_{eE} is the cathode temperature; v_{nB} is the neutral velocity at injection; α_B is the anomalous diffusion coefficient; $\tilde{\nu}_w$ is a dimensionless parameter for the wall losses model[59] ; T_{SEE} corresponds to the electron temperature yielding 100% of secondary electron emission (SEE) for the specific wall material used; a_w is the accommodation factor; and L_{m1} and L_{m2} are the characteristic lengths of variation of the magnetic field profile in the channel and in the plume respectively. The discharge current, I_d, and electron temperature at the anode, T_{eB}, are outputs of the simulation. In the reference case, these result in $I_d = 5.4$A and $T_{eB} = 2.9$ eV.

Different operating conditions are obtained through several parametric variations with respect to the reference case on the following parameters: discharge potential, V_d; mass flow rate, $\dot{m}$; channel length, L_{ch}; and gradient of magnetic field inside the channel, L_{m1}. For each parametric variation, Table 4 shows the value of the operation parameters that are modified, being the maximum magnetic field optimized for each case, and remaining the rest of parameters as in Table 1 . Details about the trends of the main properties of the Hall discharge observed in those parametric variations are provided elsewhere[60] .

Table 1. Main simulation parameters of the SPT-100 Hall thruster used as reference for the simulations.

$\dot{m}$	4.75 mg/s	V_d	300 V
B_{max}	230 G	x_{max}	25 mm
L_{ch}	25 mm	L_{AE}	33.5 mm
d_c	15 mm	R	42.5 mm
T_{eE}	5 eV	v_{nB}	300 m/s
α_B	0.094	$\tilde{\nu}_w$	0.17
T_{SEE}	30 eV	a_w	0.85
L_{m1}	15 mm	L_{m2}	5 mm

A. Results for reference solution

The stability of the reference solution in the high-frequency range is analysed in this section with the dispersion relation derived previously. Moreover, a comparison of the results obtained in experiments and with the simplified dispersion relations presented above is also carried out. The following dispersion relations (or models) are considered in this analysis:

- **Model 0**, where only the base terms are considered, corresponds to Eq. (10) above.
- **Model 1**, similar to the one used by Litvak *et al.*[4] and by Kapulkin *et al.*[6] , where the terms due to plasma density and magnetic field gradients are kept together with the base terms, corresponds to Eq. (13) above.
- **Model 2**, equivalent to the one used by Kapulkin *et al.*[7] , where ion dynamics are kept in the formulation together with the base terms, corresponds to Eq. (14) above.
- **Model 3**, where all terms due to plasma density and magnetic field gradients as well as ion dynamics and electron collisions are considered, corresponds to the dispersion relation developed in this study and given by Eq. (9) above.

Note that in all models the boundary conditions are $\phi_1 = 0$ at the extremes of the simulation domain, as self-excited oscillations are looked for and therefore no external perturbation on the discharge voltage is applied. Note as well that the solution method and its implementation have been validated against the results previously obtained by Kapulkin *et al.*[7] for simple background states.

Table 2 shows the oscillation frequency, $f = \omega_{re}/2\pi$, growth rate, $\omega_{im}/2\pi$ and phase speed, $v_y = \omega_{re}/k$, obtained from the high-frequency stability analysis of the reference solution using the different models described above for an oscillation with $m = 1$, where m is the wave mode number defined as $m = -k/R$. Note that m can only have integer values due to azimuthal continuity conditions and by definition is positive when the oscillation travels in the **E**x**B** direction (i.e., $k < 0$, $\omega_{re} > 0$).

Table 2. Results of the stability analysis for the reference solution using different models for a $m = 1$ oscillation.

	Model 0	Model 1	Model 2	Model 3
Frequency (MHz)	4.4	4.3	4.4	3.6
Growth-rate (MHz)	0.41	0.02	0.39	6.5
Phase speed (km/s)	−1182	−1163	−1188	−971

As can be seen in Table 2, all four models yield unstable oscillations (i.e., positive growth rate) rotating in the +**E**x**B** direction with an oscillation frequency in the range observed in experiments (1-10MHz). Most models yield similar results, but, however, Model 3 yields a frequency slightly smaller than the rest. Note that Model 3 combines the effects of plasma density and magnetic field gradients and of ion dynamics, which are accounted for separately in Model 1 and Model 2 respectively, and adds the effect of electron collisions. Based on the values of oscillation frequency in Table 2, it seems that the effect of electron collisions is not negligible and must be included in the formulation. In the reference background solution considered, the lower hybrid frequency, $f_{LH} = \sqrt{\omega_i \omega_e}/2\pi$, at the location of the maximum magnetic field (i.e., thruster channel exit) is $f_{LHmax} = 1.3$ MHz and decreases up to an order of magnitude near the anode and in the plume as the magnetic field decreases. This means that the resonance introduced in the formulation by ion dynamics through the term $(\omega^2 - \omega_{LH}^2)$ does not affect the first order solution since that term never vanishes for those frequencies.

Table 3 shows the frequency and phase speed obtained from the high-frequency stability analysis of the reference solution using Model 3 for different wave mode numbers m. It can be observed that the oscillation frequency scales linearly with the wave mode number and the phase speed is roughly constant. The linear relation between ω and k, as mentioned above, is also measured experimentally[1] . Moreover, oscillations with wave mode numbers $m > 1$ are also observed in experiments[1,4] .

Table 3. Results of the stability analysis for the reference background state using different wave mode numbers ($m = 1$, $m = 2$, $m = 3$, $m = 4$, $m = 6$) using the dispersion relation of Model 3.

	$m = 1$	$m = 2$	$m = 3$	$m = 4$	$m = 5$
Frequency (MHz)	3.6	7.1	10.3	13.7	17.2
Phase speed (km/s)	−971	−943	−920	−917	−916

Figs. 1-4 show for the reference background state the profiles of the plasma variables of the zero-th order solution $(n_0(x), B_0(x), v_{ey0}(x))$ entering the dispersion relations, together with the profile of the perturbed electric potential, $\phi_1(x)$, obtained from the solution of the different dispersion relations for an $m = 1$ oscillation. Note that the size of ϕ_1 does not result from the linear analysis, but is set artificially to a maximum of 100 mV, as observed in experiments[1] .

The profile of B_0 reproduces those used normally in conventional Hall thrusters, while that of n_0 is a result of the ionization and acceleration processes taking place in the Hall discharge. The profile of v_{ey0} shows a maximum in the area of highest electric field as the **ExB** drift is also maximum there, but v_{ey0} also increases towards the anode as a consequence of the electron pressure. Moreover, a discontinuity in the slope of the profile of v_{ey0} is observed in the plume due to the change of the dominant term in electron conductivity, from Bohm diffusion to near wall conductivity.

Even if in Table 2 the oscillation frequency is similar for Models 0, 1 and 2, Figs. 1-3 show important differences in the shape of $\phi_1(x)$. This indicates that the impact of gradients and ion dynamics is important in the first order solution. This is also confirmed by the larger differences in the oscillation frequency computed with Models 0 to 3 for the various operating conditions listed in Table 4. In particular, in Fig. 3 it is possible to observe that adding plasma density and magnetic field gradients in Model 1 cause the perturbation of electric field to be concentrated in the near plume, as observed normally in experiments[5,11] . This is also observed in Fig. 4 for the solution of ϕ_1 obtained with Model 3. Moreover, this area also verifies the condition $d/dx(\ln n_0/B_0) > 0$, in agreement with the local stability analysis of Esipchuk and Tilinin[2] .

Fig. 5 shows the 2D contour maps in the $x - y$ space at given t of the perturbations of electric potential, ϕ_1, plasma density, n_{e1}, and electron axial velocity, v_{ex1}, obtained with Model 3 for the reference background solution. It also shows the net electron axial current resulting from oscillations, Δj_{ex}, due to the correlation between n_{e1} and v_{ex1}. From these plots, it is possible to observe that the perturbations in plasma density are even more localized around the maximum magnetic field, this is, maximum electron gyro-frequency, ω_e. The evolution with time is characterized by the azimuthal motion of the structure shown in Fig. 5 .

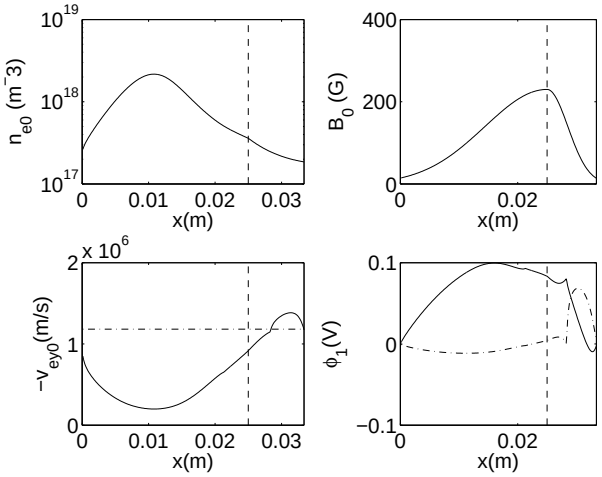

Figure 1. Axial profiles of the background solution (plasma density, n_0; magnetic field, B_0; and azimuthal electron velocity, $-v_{ey0}$, with the sign reverted to have positive values) and profile of the solution for the perturbed electric potential, ϕ_1, of the dispersion relation corresponding to Model 0. The vertical dashed line corresponds to the channel exit, where the maximum magnetic field is located. In the plot of v_{ey0} the horizontal dashed-dotted line corresponds to the value of the phase speed of the oscillation. In the plot of ϕ_1 the continuous and dashed-dotted lines correspond to the real and imaginary parts of ϕ_1 respectively.

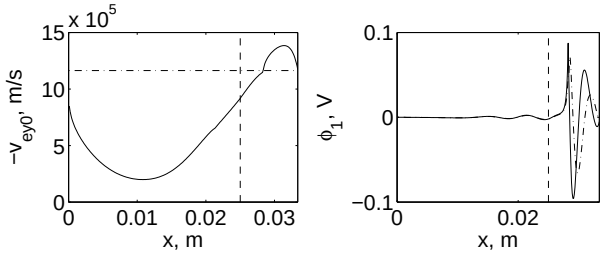

Figure 2. Same as Fig. 1 for the results obtained with Model 1.

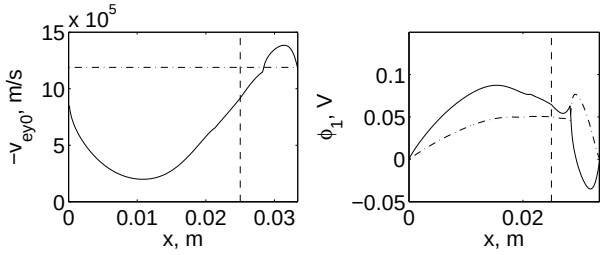

Figure 3. Same as Fig. 1 for the results obtained with Model 2.

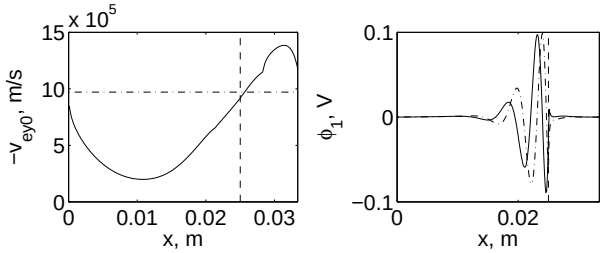

Figure 4. Same as Fig. 1 for the results obtained with Model 3.

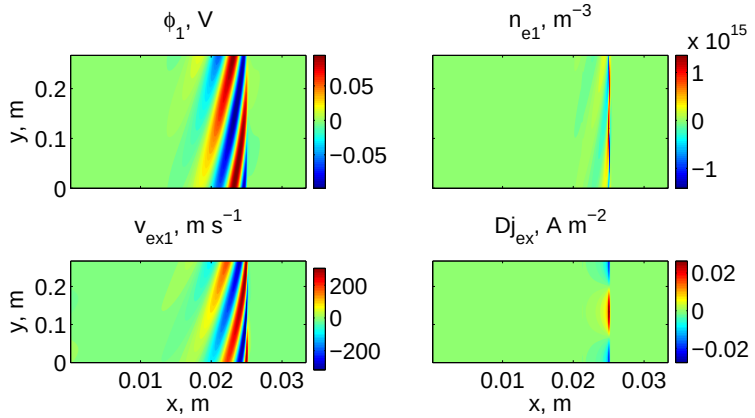

Figure 5. 2D Contour maps in the $x-y$ space at given t of the perturbations associated to the oscillation in Fig. 4 with Model 3. Variables represented: electric potential, ϕ_1; plasma density, n_{e1}; electron axial velocity, v_{ex1}; and net electron axial current from oscillations, Δj_{ex}.

B. Parametric variations

Table 4 shows the frequency of $m = 1$ oscillations obtained with the different models presented in the previous section for several operating conditions derived from the parametric variations on V_d, $\dot{m}$, L_{ch}, and L_{m1} described previously[60] . The order of magnitude of the oscillation frequency in most cases lies in the 2-5MHz range, in agreement with experiments.

The comparison among the results obtained with the different models shows that all terms (gradients, ion dynamics and electron collisions) play a certain role in the computation of the oscillation frequency, and therefore, it is necessary to use Model 3 to account for all effects. The comparison of the columns in Table 4 corresponding to Model 0 and Model 2, differing only in the presence of ion dynamics in Model 2, reveals that the impact of ion dynamics is not very relevant since the values of oscillation frequency obtained with those two models are fairly similar in most cases. On the other hand, the comparison of the results for Model 0 and Model 1 indicates that the gradients of plasma density and magnetic field are more relevant, especially due to the factor ω_e of one of the terms associated to those gradients. Finally, electron collisions play also an important role based on the differences between the results of Model 3 and the rest of models.

The phase speed of the oscillation is expected to scale roughly as the velocity of the **E**x**B** drift, this is, as E/B, where E and B are typical values of electric and magnetic field. As mentioned above, in the case of Model 0, these correspond to the point where the condition $d^2v_{ey0}/dx^2 = 0$ is met. In the case of Model 1, this condition is transformed into $\Lambda = 0$. For Model 2 the condition is again $d^2v_{ey0}/dx^2 = 0$, but two possible resonances may occur, $\omega = kv_{ey0}$ or $\omega^2 = \omega_e\omega_i$. However, for Model 3 deriving such condition is not straightforward due to the various terms appearing in the dispersion relation, but still the resulting phase speed is expected to scale as E/B. Thus, both the discharge voltage, V_d, and the maximum magnetic field, B_{max}, determine mostly the value of phase speed, v_y, and frequency, f. However, the latter values are also affected by: the profiles of electric potential and magnetic field, through the definition of the profile of v_{ey0}; and the plasma density gradient and the electron collisions, through the various terms appearing in the dispersion relation. Thus, it is not possible to establish a direct relationship between V_d and B_{max}, and v_y and f.

The following comments are based on the column corresponding to Model 3 in Table 4:

- as the discharge voltage increases, the oscillation frequency increases. However, the increase is not linearly proportional since as part of the parametric variation the magnetic field is increased as $B_{max} \propto V_d^p$, with $p \approx 0.5$, in order to keep the Hall discharge in optimum operation[60] .

- as the mass flow increases, the oscillation frequency remains approximately constant since V_d is fixed and B_{max} remains fairly constant.

- as the channel length is increased, the oscillation frequency increases as well since V_d is fixed and B_{max} is decreased to maintain the Hall discharge in optimum conditions.

- as the gradient of the magnetic field is increased (i.e., L_{m1} is decreased), the oscillation frequency decreases since V_d is fixed and B_{max} is increased as part of the parametric variation to keep optimum operation conditions.

In all cases analysed with Model 3 except one, the oscillation frequency is above the maximum lower hybrid frequency in the channel, linked to the maximum magnetic field. This indicates that the resonance introduced by ion dynamics through the term $(\omega^2 - \omega_{LH}^2)$ in the dispersion relation does not normally play any role in the azimuthal instability.

Only in the case B4 analysed with Model 3, the oscillation frequency is $f = 0.32$ Mhz, lower than the maximum hybrid-lower frequency ($f_{LHmax} = 1.41MHz$), but greater than the minimum value. Thus the condition $\omega = \omega_{LH}$ occurs inside the channel in this case. Fig. 9 shows the axial profiles of the background state and of the solution of ϕ_1 for case B4. Contrary to all other cases where the oscillation is located in the area around the maximum electric and magnetic fields, in this case B4, the oscillation is located in the centre of the channel, where the resonance takes place as shown in Fig. 7. A similar behaviour is observed with case D3 in Table 4 when analysed with Model 2 as shown in Fig. 8. These are the only two cases among those analysed where the condition $\omega = \omega_{LH}$ takes place instead of $\omega = kv_{ey0}$. Models 0 and 1 do not include ion dynamics and thus cannot show such behaviour, as verified by the corresponding columns in Table 4.

Table 4. Parameters of the background solutions under analysis (A, B, C and D refer to the parametric variations on V_d, $\dot{m}$, L_{ch}, and L_{m1} respectively), oscillation frequency (f, MHz) for a $m = 1$ oscillation, and maximum lower-hybrid frequency (f_{LHmax}, MHz) for each of the operating conditions

	Parameter	Parameter	Model 0	Model 1	Model 2	Model 3	
Case	V_d, V	B_{max}, G	f, MHz	f, MHz	f, MHz	f, MHz	f_{LHmax}, MHz
A1	200	179	3.39	3.28	3.44	2.98	1.30
REF	300	230	4.42	4.34	4.44	3.63	1.01
A2	500	313	4.68	5.76	4.71	4.51	1.77
A3	700	383	5.33	6.80	5.40	5.22	2.17
Case	$\dot{m}, mg/s$	B_{max}, G	f, MHz	f, MHz	f, MHz	f, MHz	f_{LHmax}, MHz
B1	3.3	225	4.12	4.01	4.14	3.55	1.28
B2	4	226	4.34	4.27	4.38	3.62	1.28
REF	4.8	230	4.42	4.34	4.44	3.63	1.30
B3	7	241	3.63	4.49	3.68	3.60	1.37
B4	8.5	249	3.55	4.54	3.60	0.32	1.41
Case	L_{ch}, mm	B_{max}, G	f, MHz	f, MHz	f, MHz	f, MHz	f_{LHmax}, MHz
C1	14	401	2.93	2.69	1.40	2.54	0.80
REF	25	230	4.42	4.34	4.44	3.63	1.05
C2	26	217	4.55	4.46	4.57	3.76	1.30
C3	42	141	5.57	5.30	5.59	4.54	2.14
Case	L_{m1}, mm	B_{max}, G	f, MHz	f, MHz	f, MHz	f, MHz	f_{LHmax}, MHz
D1	30	142	5.40	5.16	5.41	4.48	2.28
D2	19	185	4.90	4.74	4.92	4.05	1.30
REF	15	230	4.42	4.34	4.44	3.63	1.23
D3	9	377	3.06	2.72	0.18	2.59	0.80

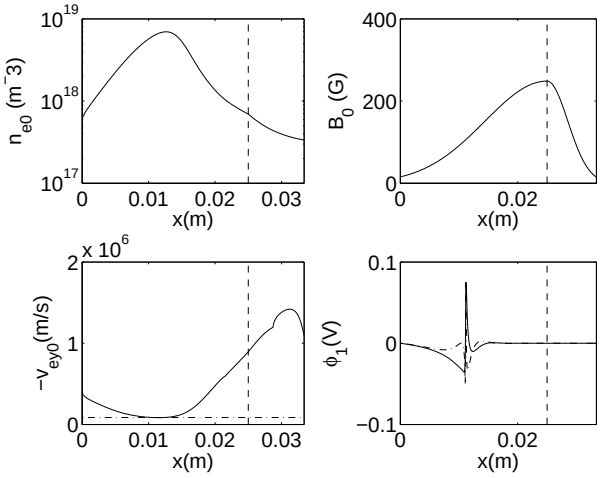

Figure 6. Same as Fig. 1 with background solution B4 and Model 3.

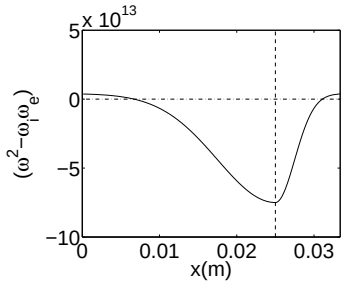

Figure 7. Plot of $\omega_{re}^2 - \omega_e\omega_i$ with background solution B4 and Model 3.

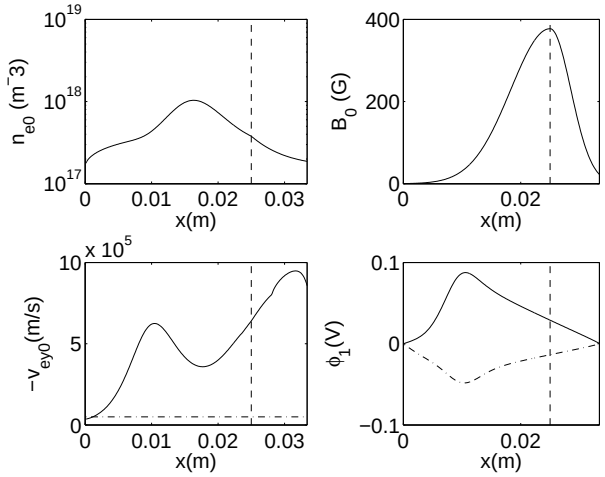

Figure 8. Same as Fig. 1 with background solution D3 and Model 2.

V. Contribution to anomalous diffusion

Aside from the numerical analysis of electron-drift waves carried out in the previous section, it is possible to compute the electron transport due to oscillations using the same method as in previous low frequency analyses[61] . This requires using as inputs the perturbations of plasma density and electron axial velocity, n_{e1} and v_{ex1}, from Eqs. (6), in order to compute the equivalent anomalous diffusion coefficient, $\alpha_A(x)$, as defined in Ref. [61], and the oscillation-based electron current as $I_{e1} = -1/2\Re(en_{e1}v_{ex1}^*)A$, where A is the cross-section of the thruster and * refers to the complex conjugate.

Figs. 9 and 10 show respectively the oscillation-based electron current and the equivalent anomalous diffusion coefficient for the reference background state and the perturbed solution computed with Model 3. The resulting maximum electron current is positive, but well below the mA level. Note in any case that this computation is affected by the assumed size of the linear perturbations, set to 100mV based on experimental results[1] for the maximum electric potential perturbation. Only in case the perturbation were 100 times larger (e.g., 10V in electric potential), the oscillation-based electron transport would be in the order of 1A. However, such large electric potential oscillations are not normally observed experimentally in the high-frequency range under analysis. Similar results in terms of oscillation-based transport are obtained in all operating conditions shown in Table 4 and in all wave mode numbers in Table 3.

Thus, it seems that the contribution to electron conductivity from these high-frequency electron-drift waves is not relevant, not even in the region of high electric and magnetic fields, where the oscillation is normally observed.

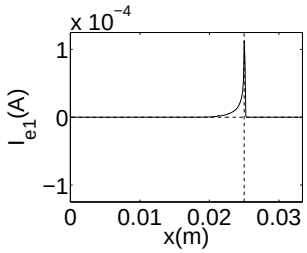

Figure 9. Oscillation-based electron current due to high-frequency oscillations computed with Model 3 for the reference case. The vertical dashed-line corresponds to the channel exit.

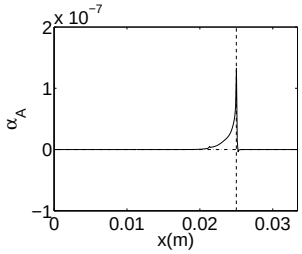

Figure 10. Equivalent anomalous diffusion coefficient due to high-frequency oscillations computed with Model 3 for the reference case. The vertical dashed-line corresponds to the channel exit.

VI. Conclusions

In first place an in-depth literature review of high-frequency oscillations in Hall thrusters has been performed with focus on electron-drift oscillations commonly observed in experiments. In second place, an axial-azimuthal global stability analysis of the Hall discharge in the high-frequency range (1-10MHz) has been carried out with the goal of characterizing numerically the electron-drift waves observed experimentally[1,3,5,11] and evaluating the role of those oscillations in the anomalous diffusion process in Hall thrusters.

To that end a dispersion relation has been developed accounting for ion dynamics, gradients of plasma density and magnetic field, and electron collisions. The resulting dispersion relation is a generalization of others developed in the past[4,6,7] , which consider some of those terms separately.

As part of the numerical study the dispersion relation has been solved for axial profiles of the Hall discharge computed with the 1D model of Ahedo *et al.*[59] . As expected, results show the presence of high-frequency oscillations rotating in the +**E**x**B** direction with a velocity in the order of the **E**x**B** drift around the region of maximum electric and magnetic fields. Experimental trends on the properties of electron-drift waves have been verified through simulations, such as the variation of the oscillation frequency with discharge voltage or magnetic field. Moreover, the linear relation between oscillation frequency and wave number observed in experiments has also been verified in the simulations.

The evaluation of the electron current due to these electron-drift oscillations seems to indicate that their contribution to the electron perpendicular transport is residual, localized in the region of maximum electric and magnetic fields, and too small to justify the anomalous diffusion typically observed in Hall thrusters.

Acknowledgments

Support to D. Escobar has been provided by the Air Force Office of Scientific Research, Air Force Material Command, USAF, under Grant No. FA8655-13-1-3033. Support to E. Ahedo has come from Spain's R&D National Plan (Proyect ESP-2013-41052)

References

[1]A. Lazurenko, V. Krasnoselskikh, and A. Bouchoule, "Experimental Insights Into High-Frequency Instabilities and Related Anomalous Electron Transport in Hall Thrusters," *IEEE Transactions on Plasma Science*, vol. 36, no. 5 Part 1, pp. 1977–1988, 2008.

[2]Y. Esipchuk and G. Tilinin, "Drift instability in a Hall-current plasma accelerator," *Sov. Physics-Tech. Physics*, vol. 21, no. 4, pp. 417–423, 1976.

[3]G. Guerrini and C. Michaut, "Characterization of high frequency oscillations in a small Hall-type thruster," *Physics of Plasmas*, vol. 6, p. 343, 1999.

[4]A. Litvak and N. Fisch, "Rayleigh instability in Hall thrusters," *Physics of Plasmas*, vol. 11, p. 1379, 2004.

[5]A. Knoll and M. Cappelli, "Experimental Characterization of High Frequency Instabilities within the Discharge Channel of a Hall Thruster ," in *Proceedings of the 31st International Electric Propulsion Conference*, 2009.

[6]A. Kapulkin, J. Ashkenazy, A. Kogan, G. Appelbaum, D. Alkalay, and M. Guelman, "Electron instabilities in Hall thrusters: modelling and application to electric field diagnostics," in *Proceedings of the 28th International Electric Propulsion Conference*, 2003.

[7]A. Kapulkin and M. Guelman, "Lower-hybrid instability in Hall thruster," in *Proceedings of the 29th International Electric Propulsion Conference*, 2005.

[8]E. Ahedo, J. Gallardo, and M. Martinez-Sanchez, "Model of the plasma discharge in a hall thruster with heat conduction," *Physics of Plasmas*, vol. 9, p. 4061, 2002.

[9]G. Tilinin, "High-frequency plasma waves in a Hall accelerator with an extended acceleration zone," *Soviet Physics-Technical Physics*, vol. 22, no. 8, pp. 974–978, 1977.

[10]A. Litvak, Y. Raitses, and N. Fisch, "Experimental studies of high frequency oscillations in Hall thrusters," in *Proceedings of the 38th Joint Propulsion Conference*, 2002.

[11]A. Litvak, Y. Raitses, and N. Fisch, "Experimental studies of high-frequency azimuthal waves in Hall thrusters," *Physics of Plasmas*, vol. 11, p. 1701, 2004.

[12]M. Prioul, A. Bouchoule, S. Roche, L. Magne, D. Pagnon, M. Touzeau, and P. Lasgorceix, "Insights on physics of Hall thrusters through fast current interruptions and discharge transients," in *Proceedings of the 27th International Electric Propulsion Conference*, 2001.

[13]A. Lazurenko, V. Vial, A. Bouchoule, M. Prioul, J. Adam, A. Heron, and G. Laval, "Characterization of microinstabilities in a Hall thruster plasma: experimental and PIC code simulation results, physical interpretation and impact on transverse electron transport," in *Proceedings of the 29th International Electric Propulsion Conference*, 2003.

[14]A. Lazurenko, V. Vial, A. Bouchoule, L. Albarede, and M. Dudeck, "High-frequency instabilities and low-frequency dynamics in Hall thruster plasma," in *Proceedings of the 40th Joint Propulsion Conference*, 2004.

[15]A. Lazurenko, V. Vial, M. Prioul, and A. Bouchoule, "Experimental investigation of high-frequency drifting perturbations in Hall thrusters," *Physics of Plasmas*, vol. 12, p. 013501, 2005.

[16]A. Lazurenko, L. Albarède, and A. Bouchoule, "High-frequency Instabilities in Hall-effect Thrusters: Correlation with the Discharge Current and Thruster Scale Impact," in *Proceedings of the 29th International Electric Propulsion Conference*, 2005.

[17]A. Lazurenko, L. Albarede, and A. Bouchoule, "Physical characterization of high-frequency instabilities in Hall thrusters," *Physics of Plasmas*, vol. 13, p. 083503, 2006.

[18]G. Coduti, A. Lazurenko, S. Mazouffre, M. Dudeck, T. De Wit, C. Cavoit, V. Krasnoselskikh, and A. Bouchoule, "Investigation of electron transport properties in Hall thrusters through measurements of magnetic field fluctuations," in *Proceedings of the 30th International Electric Propulsion Conference*, 2007.

[19]A. Lazurenko, T. de Wit, C. Cavoit, V. Krasnoselskikh, A. Bouchoule, and M. Dudeck, "Determination of the electron anomalous mobility through measurements of turbulent magnetic field in Hall thrusters," *Physics of Plasmas*, vol. 14, p. 033504, 2007.

[20]A. Lazurenko, G. Coduti, S. Mazouffre, and G. Bonhomme, "Dispersion relation of high-frequency plasma oscillations in hall thrusters," *Physics of Plasmas*, vol. 15, p. 034502, 2008.

[21]A. Morozov, Y. Esipchuk, A. Kapulkin, V. Nevrovskii, and V. Smirnov, "Effect of the magnetic field on a closed-electron-drift accelerator," *Soviet Physics-Tech. Physics*, vol. 17, no. 3, pp. 482–487, 1972.

[22]A. Litvak and N. Fisch, "Resistive instabilities in Hall current plasma discharge," *Physics of Plasmas*, vol. 8, p. 648, 2001.

[23]A. Knoll, C. Thomas, N. Gascon, and M. Cappelli, "Experimental Investigation of High Frequency Plasma Oscillations within Hall Thrusters," in *Proceedings of the 42nd Joint Propulsion Conference*, 2006.

[24]D. Tomilin and O. Gorshkov, "Role of High-Frequency Waves in Process of Electron Conductivity in SPT with High Specific Impulse," in *Proceedings of the 32nd International Electric Propulsion Conference*, 2011.

[25]L. Albarede, S. Mazouffre, A. Bouchoule, and M. Dudeck, "Low-frequency electron dynamics in the near field of a Hall effect thruster," *Physics of Plasmas*, vol. 13, p. 063505, 2006.

[26]J. Kurzyna, S. Mazouffre, A. Lazurenko, L. Albarède, G. Bonhomme, K. Makowski, M. Dudeck, and Z. Peradzyński, "Spectral analysis of Hall-effect thruster plasma oscillations based on the empirical mode decomposition," *Physics of Plasmas*, vol. 12, p. 123506, 2005.

[27]J. Kurzyna, K. Makowski, Z. Peradzyński, A. Lazurenko, S. Mazouffre, G. Coduti, and M. Dudeck, "Current and Plasma Oscillation Inspection in PPS-X000 HET Thruster - EMD Approach," in *Proceedings of the 30th International Electric Propulsion Conference*, 2007.

[28]J. Kurzyna, K. Makowski, Z. Peradzyński, A. Lazurenko, S. Mazouffre, and M. Dudeck, "Where is the breathing mode ? High voltage Hall effect thruster studies with EMD method," in *Proceedings of the International Conference on Research and Applications of Plasmas*, 2008.

[29]G. Bonhomme, C. Enjolras, and J. Kurzyna, "Characterization of Hall Effect Thruster Plasma Oscillations based on the Hilbert-Huang Transform," in *Proceedings of the 29th International Electric Propulsion Conference*, 2005.

[30]G. Bonhomme, N. Lemoine, F. Brochard, A. Lazurenko, S. Mazouffre, and M. Dudeck, "Characterization of High Frequency plasma oscillations in a Hall Effect Thruster," in *Proceedings of the 30th International Electric Propulsion Conference*, 2007.

[31]J. Adam, A. Heron, and G. Laval, "Study of stationary plasma thrusters using two-dimensional fully kinetic simulations," *Physics of Plasmas*, vol. 11, p. 295, 2004.

[32]L. Garrigues and P. Coche, "A two-dimensional (azimuthal-axial) particle-in-cell model of a hall thruster," in *Proceedings of 33rd International Electric Propulsion Conference*, 2013.

[33]P. Coche and L. Garrigues, "A two-dimensional (azimuthal-axial) particle-in-cell model of a hall thruster," *Physics of Plasmas*, vol. 21, no. 2, p. 023503, 2014.

[34]J. Adam, J. Boeuf, N. Dubuit, M. Dudeck, L. Garrigues, D. Gresillon, A. Heron, G. Hagelaar, V. Kulaev, N. Lemoine, *et al.*, "Physics, simulation and diagnostics of hall effect thrusters," *Plasma Physics and Controlled Fusion*, vol. 50, p. 124041, 2008.

[35]S. Tsikata, N. Lemoine, V. Pisarev, and D. Grésillon, "Dispersion relations of electron density fluctuations in a hall thruster plasma, observed by collective light scattering," *Physics of Plasmas*, vol. 16, p. 033506, 2009.

[36]S. Tsikata, D. Gresillon, C. Honore, V. Pisarev, and N. Lemoine, "Small-scale density fluctuation modes in a Hall plasma thruster: experimental studies via collective light scattering," in *Proceedings of the 31st International Electric Propulsion Conference*, 2009.

[37]S. Tsikata, N. Lemoine, V. Pisarev, and D. Gresillon, "Dispersion relations of electron density fluctuations in a hall thruster plasma, observed by collective light scattering," *Physics of Plasmas*, vol. 16, p. 033506, 2009.

[38]S. Tsikata, C. Honore, D. Gresillon, A. Heron, N. Lemoine, and J. Cavalier, "The small-scale high-frequency ExB instability and its links to observed features of the Hall thruster discharge ," in *Proceedings of the 33rd International Electric Propulsion Conference*, 2013.

[39]M. Hirakawa and Y. Arakawa, "Particle simulation of plasma phenomena in Hall thrusters," in *Proceedings of the 24th International Electric Propulsion Conference*, 1995.

[40]M. Hirakawa, "Electron transport mechanism in a Hall thruster," in *Proceedings of the 25th International Electric Propulsion Conference*, 1997.

[41]M. Cappelli, N. Meezan, and N. Gascon, "Transport physics in Hall plasma thrusters," in *Proceedings of the 40th AIAA Aerospace and Sciences Meeting and Exhibit*, 2002.

[42]A. Ducrocq, J. Adam, A. Héron, and G. Laval, "Theoretical analysis of anomalous conductivity in Hall Effect Thrusters," in *Proceedings of the 29th International Electric Propulsion Conference*, 2005.

[43]C. Honore, S. Tsikata, D. Gresillon, A. Heron, J. Cavalier, and N. Lemoine, "Hall Thruster small scale plasma fluctuations: Qualifying 2D PIC Simulations against Collective Scattering Experimental Data," in *Proceedings of the 32nd International Electric Propulsion Conference*, 2011.

[44]P. Coche and L. Garrigues, "Study of stochastic effects in a Hall effect thruster using a test particles Monte-Carlo model," in *Proceedings of the 32nd International Electric Propulsion Conference*, 2011.

[45]C. M. Lam, A. K. Knoll, M. A. Cappelli, and E. Fernandez, "Two-Dimensional (z-θ) Simulations of Hall Thruster Anomalous Transport," in *Proceedings of the 31st International Electric Propulsion Conference*, 2009.

[46]A. Knoll, N. Gascon, and M. Cappelli, "Numerical simulation of high frequency wave coupling within a Hall thruster," in *Proceedings of the 43rd Joint Propulsion Conference*, 2007.

[47]V. Baranov, Y. Nazarenko, and V. Petrosov, "New conceptions of oscillation mechanisms in the accelerator with closed drift of electrons," in *Proceedings of the 24th International Electric Propulsion Conference*, 1995.

[48]V. Baranov, Y. Nazarenko, V. Petrosov, A. Vasin, and Y. Yashnov, "Electron drift oscillations outside acceleration zone of accelerator with closed electron drift," in *Proceedings of the 24th International Electric Propulsion Conference*, 1995.

[49]V. Baranov, Y. Nazarenko, V. Petrosov, and A. Vasin, "Electron conductivity in ACD," in *Proceedings of the 26th International Electric Propulsion Conference*, 1999.

[50]C. Thomas and M. Cappelli, "Fluctuation-induced transport in the Hall plasma accelerator," in *Proceedings of the 42nd Joint Propulsion Conference*, 2006.

[51]C. Thomas, *Anomalous electron transport in the Hall-effect thruster*. PhD thesis, Stanford University, 2006.

[52]R. Spektor, "Quasi-Linear Analysis Of Anomalous Electron Mobility Inside A Hall Thruster," in *Proceedings of the 30th International Electric Propulsion Conference*, 2007.

[53]C. Boniface, L. Garrigues, G. Hagelaar, J. Boeuf, D. Gawron, and S. Mazouffre, "Anomalous cross field electron transport in a Hall effect thruster," *Applied Physics Letters*, vol. 89, p. 161503, 2006.

[54]A. Ducrocq, J. Adam, A. Héron, and G. Laval, "High-frequency electron drift instability in the cross-field configuration of Hall thrusters," *Physics of Plasmas*, vol. 13, p. 102111, 2006.

[55]A. Ducrocq, *Role des instabilites electroniques de derive dans le transport electronique du propulseur a efet Hall.* PhD thesis, Ecole Polytechnique, 2006.

[56]A. Kapulkin and V. Prisnyakov, "Dissipative method of suppression of electron drift instability in SPT," in *Proceedings of the 24th International Electric Propulsion Conference*, 1995.

[57]A. Kapulkin, E. Behar, and Y. Raitses, "Ion beam instability in hall thrusters," in *Proceedings of 33rd International Electric Propulsion Conference*, 2013.

[58]D. Escobar and E. Ahedo, "Analysing the azimuthal spoke oscillation of Hall thrusters via numerical simulation," in *Proceedings of the 50th Joint Propulsion Conference*, 2014.

[59]E. Ahedo, J. Gallardo, and M. Martinez-Sanchez, "Effects of the radial plasma-wall interaction on the hall thruster discharge," *Physics of Plasmas*, vol. 10, p. 3397, 2003.

[60]E. Ahedo and D. Escobar, "Influence of design and operation parameters on hall thruster performances," *Journal of applied physics*, vol. 96, p. 983, 2004.

[61]D. Escobar and E. Ahedo, "Global stability analysis of azimuthal oscillations in hall thrusters," *IEEE Transactions on Plasma Science*, vol. 43, no. 1, pp. 149–157, 2015.